Nonambipolar Transport due to Electrons with 3D Resistive Response in the KSTAR Tokamak

S. M. Yang, J.-K. Park, Yong-Su Na, Z. R. Wang, W. H. Ko, Y. In, J. H. Lee, K. D. Lee, and S. K. Kim

Phys. Rev. Lett. **123**, 095001 — Published 29 August 2019

DOI: 10.1103/PhysRevLett.123.095001

Non-ambipolar transport due to electrons with 3D resistive response in the KSTAR tokamak

S.M. Yang,[1] J.-K. Park,[2,∗] Yong-Su Na,[1,†] Z.R. Wang,[2] W.H. Ko,[3] Y. In,[4] J.H. Lee,[3] K.D. Lee,[3] and S.K. Kim[1]

[1]*Department of Nuclear Engineering, Seoul National University, Seoul 08826, Republic of Korea*
[2]*Princeton Plasma Physics Laboratory, Princeton, New jersey 08543, USA*
[3]*National Fusion Research Institue, Daejeon 305-333, Republic of Korea*
[4]*Ulsan National Institute of Science and Technology, Ulsan 689-798, Republic of Korea*

(Dated: July 19, 2019)

A small non-axisymmetric (3D) magnetic field can induce non-ambipolar transport of the particle species confined in a tokamak and thus a significant change of plasma rotation. This process can be in a favor of instability control in the region where the tokamak plasma is sufficiently collisional and resistive, as observed in the applications of $n = 1$ resonant magnetic perturbations to the KSTAR tokamak. The plasma rotation can be globally accelerated due to radially drifting electrons and constrained to the electron root, if the radial transport is enhanced by amplified 3D response. This mechanism is verified by a kinetically self-consistent magnetohydrodynamic modeling for both response and transport, which offers the quantitative explanations on the internal n=1 structure detected by electron-cyclotron-emission imaging and the co-current plasma spinning observed in the experiments.

PACS numbers:

A tokamak relies on the axisymmetric magnetic fields to confine fusion plasmas. Recently a great deal of attention has been drawn to the use of a small non-axisymmetric (3D) magnetic perturbation $\delta\vec{B}$, due to its significant impact on toroidal rotation and thereby plasma confinement [1–3] and stability [4–7]. An invariably caused effect by the broken symmetry is the radial drift of particles across magnetic surfaces to conserve the orbital action. This process, as well known by neoclassical toroidal viscousity (NTV) transport [8–13], is fundamentally independent of each species, i.e. non-ambipolar, resulting in the evolution of radial electric field and rotation until a new torque balance is established. Typically ions are dominant in the process as they collide less frequently and thus drift further than electrons, slowing rotation down against the direction of plasma current I_P. This is the magnetic braking effect [14–16] generally unfavorable of stability, especially if the externally driven torque is not sufficient as expected in the next step devices such as ITER [17]. In this Letter, we report a global and quiescent magnetic acceleration observed in the Korean superconducting tokamak advanced research (KSTAR) facility associated with non-ambipolar electron transport, and the validation of its mechanism using self-consistently regulated 3D resistive response simulations. It is also clearly shown that the magnetic acceleration can improve the tolerance of slowly rotating plasmas against a disruptive 3D magnetohydrodynamic (MHD) instability.

Magnetic acceleration by electron NTV can be induced in various special conditions [18–20], such as higher temperature of electrons than ions ($T_e \gg T_i$), or considerably low or high ion collisions so that the ion orbital motions are deflected rather by precession or even not periodically formed. Our study is revealing electron NTV in high-collisionality conditions where the direct applicability is limited in fusion plasmas except the ramp-up and ramp-down phase of discharges [21]. The study nonetheless implies the viability of electron NTV physics that should be applicable in wider parametric regimes including low-collisionality as has been theoretically expected for the next step devices. The electron-dominated kinematics should also be combined with strong $\delta\vec{B}$ to take its effects, as otherwise the electron NTV may be too weak to accelerate rotation. $\delta\vec{B}$ is established through plasma response to external magnetic perturbations often in fast MHD time scales but can also evolve later due to slower MHD or kinetic effects. For example, the non-ambipolar transport generates tensor pressure and can significantly change $\delta\vec{B}$ in equilibrium, which will then further modify the non-ambipolar transport until the two processes become self-consistent. We find that the magnetic acceleration observed in KSTAR is associated with resonant $\delta\vec{B}$ amplified due to resistive field penetration but self-consistently regulated by accompanying non-ambipolar electron currents, as validated by the MARS-K code [22] and electron-cyclotron-emission (ECEI) imaging diagnostics. The simulation also quantitatively explains the measured torque and rotation evolution towards a new balance between the electron and ion roots of ambipolar rotation level, strongly supporting the idea of generalized offset rotation in KSTAR proposed in [19, 20].

The KSTAR experiments introduced in Fig. 1 clearly

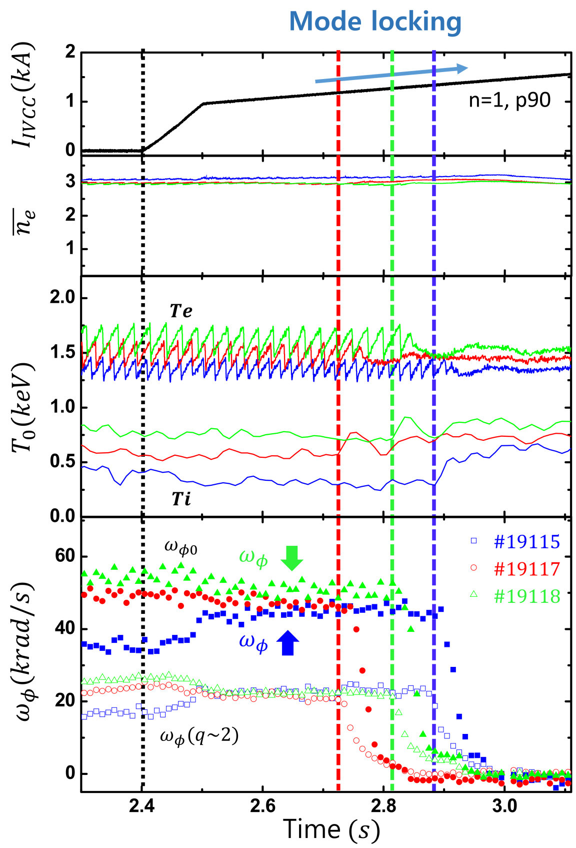

FIG. 1: (color) The time traces of main plasma parameters in KSTAR discharges. (a) Amplitude of IVCC coil currents, (b) line-averaged plasma density, (c) core electron and ion temperature, (d) toroidal rotation frequency measured at the core ($\omega_{\phi 0}$) and at the $q \sim 2$ ($\omega_\phi\,(q \sim 2)$) location.

show the acceleration of toroidal rotation due to a 3D magnetic field, and the saturation of the effect at a particular level of rotation. Here the top trace shows the applied $n = 1$ resonant magnetic field, for which the currents in 3 rows of in-vessel control coils (IVCC) are relatively shifted by 90^o toroidal angle. This 3D setting is often used to generate a resonant magnetic perturbation (RMP) to suppress the edge-localized-mode (ELM) in KSTAR [23, 24]. Here our target plasmas are heated by the co-I_P-directed neutral beam injection (NBI) with the $I_P = 0.6MA$ and the toroidal field $B_T = 2T$, which make the so-called safety factor $q_{95} \approx 5$. Another purpose of the experiments is to study the tolerance of low-torque plasmas against $n = 1$ disruptive 3D MHD instability the so-called a locked mode (LM) [25] during a period before the transition to a high-confinement (H) mode, and therefore NBI power $P_{NB} < 1MW$ is used and controlled. With the lowest $P_{NB} \sim 0.56MW$ (# 19115), one can see magnetic acceleration of rotation shown in the bottom trace, up to 30% from the core to the edge measured by charges exchange spectroscopy (CES) of the carbon impurity [26].

This co-I_P-directed acceleration of rotation due to a RMP up to 50krad/s in the core region has been never reported in a tokamak. Another interesting feature is the saturation of the rotation evolution in a particular level despite the gradual increase of the applied RMP strength. Although the rate change of the RMP strength at $t = 2.5s$ is also attributed to the slower increase of rotation, only a few % change in the rotation from that time while the RMP field is increased up to 30% is not consistent with the increased torque up to 70% expected from the standard NTV theory, i.e. $\propto \delta B^2$. As explained later, this saturation is associated with the linearly decreased torque by electrons towards the so-called electron root of rotation [8]. It is also interesting to see a slow but clearly decreasing rotation by the RMP as seen in the other two discharges, where the initial rotation was higher than the saturation level due to the slightly higher NBI power. Note that the density and temperature of thermal species are almost stationary under the RMP unlike earlier studies on electron NTV [18] or magnetic acceleration [13], until another major bifurcation called locked mode (LM) is triggered later in time.

Fig. 1 also shows that the magnetic acceleration can improve the tolerance of the low torque plasmas against LMs. The vertical dash lines for each discharge are indicating the onset of LMs, pulling down rotation to zero level everywhere as nicely measured by CES. This bifurcation is understood as the evolution of unstable magnetic islands to large size at low order rational surfaces due to the electromagnetic 3D torque against the viscous torque of rotating plasmas, dissipating toroidal momentum [27] until locked to the frame of the external 3D fields. The viscous torque and rotation at the rational surface are therefore stabilizing against the onset of LMs, enhancing the plasma tolerance against RMP, as has been validated in various devices [7, 28–32] as well as KSTAR [32]. The case #19115 had the lowest NBI power and torque injection, and therefore a much lower RMP tolerance was expected than the other two discharges. However, the RMP threshold became comparable at the time of the LM onset as can be seen in Fig. 1. In fact, the rotation at $q = 2$ became slightly higher than the other two and so was the RMP threshold at the onset (i.e. $\omega_\phi(\#19115) > \omega_\phi(\#19118) > \omega_\phi(\#19117)$), consistent with the expectation on the LMs driven across the 2/1 rational surface and stabilizing effect of $q = 2$ rotation. On the other hand, the bifurcation process observed here does not show any precursor in rotation unlike the prevailing supposition of the onset occurring after gradual rotation reduction [25, 33]. It is also interesting to see plasma confinement maintained over a couple of τ_E without rotating at all in these NBI assisted L-mode plasmas. The ion temperature is seen to increase as the LMs grow in particular for #19115, but the analysis of these non-linear behaviors is remained as future work since it

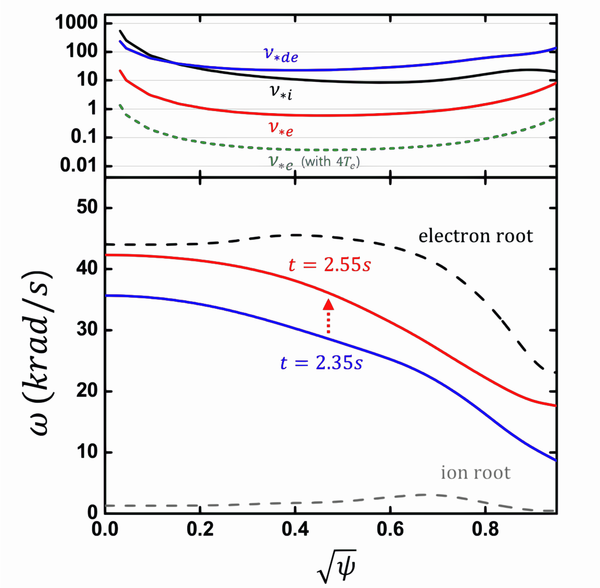

FIG. 2: (color) (a) Radial profiles of ν_{*i}, ν_{*e}, ν_{*de} for #19115 at t = 2.55 s. (b) Radial profiles of toroidal rotation frequency for #19115 at t = 2.35 s and t = 2.55 s, with electron and ion offset rate at t = 2.55 s.

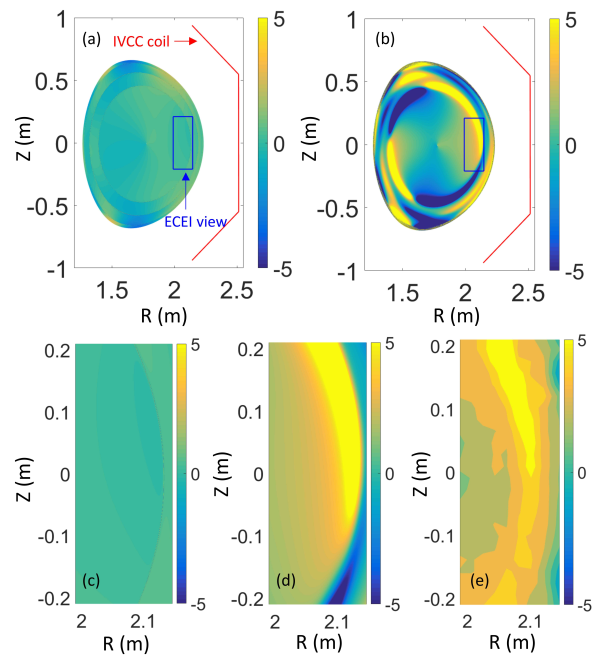

FIG. 3: (color). Comparison of the computed normal plasma displacement (mm) of #19118 in KSTAR (a), (c) without 3D resistive plasma response and (b), (d) with 3D resistive plasma response using MARS-K, and (e) estimated 2D displacement (mm) by $\xi_n = -\delta T_e/|\nabla T_e|$ [35] using ECE and electron cyclotron emission imaging data $(\delta T_e = \delta T_{e,t2} - \delta T_{e,t1})$ in #19118.

is not necessary to understand the initial acceleration.

Magnetic acceleration can occur when the applied 3D field can generate the outward transport of electrons more strongly than ions, since then the radial electric field E_r can be shifted towards positive values and the radial force balance with $\vec{E} \times \vec{B}$ will demand higher rotation to the co-I_P direction [18]. This is indeed a plausible mechanism for our observations, as will be explained here and quantitatively later. E_r is already positive as the plasmas are rotating in the co-I_P direction except for the narrow region in the edge, and thus tends to attract drifting electrons through the broken symmetry. A balance occurs at the electron root for the ambipolar E_r, which is also often called the electron NTV offset rotation [19]. The offset varies depending on the collisionality of each species. The collisional rate normalized to the bouncing frequency of trapped particles, $\nu_{*s} \equiv \epsilon^{-3/2}\nu_s/\omega_{bs}$ [8] is shown in Figure 2(a) for each ion (s=i) and electron (s=e), indicating that the ions are too collisional to complete the bounce motions. Electrons are much less collisional and in fact are mostly in the so-called $1/\nu$ collisionless regime. They are in the $1/\nu$ regime since $\nu_{*de} \equiv \nu_e/2\epsilon\omega_E \gg 1$ which means that precessional effect can be ignored overall, and can be treated as collisionless particles since $\nu_{*e}(4T_e) < 1$ except for the far edge and near the magnetic axis. The collisionless criterion $\nu_{*e}(4T_e) < 1$ can be justified by the fact that non-ambipolar transport flux in the $1/\nu$ regime is $\Gamma^{na} \propto E^4 e^{E/T_0}$ [10] and thus dominated by more energetic particles with $E \approx 4T_0$ than mean thermal ones.

The electron NTV offset rotation is then given by $\Omega_{*e} \equiv \left(\omega_\varphi + \omega_{d,e} - \omega_{d,i} - c_{t,e}\frac{dT_e}{d\psi}\right)$ [34], where $\omega_{d,s}$ is the diamagnetic rotation for each species and $c_{t,e} = 2.4$. As shown in Fig. 2(b), the offset rotation profile is greater than the rotation in #19115 indicating the feasibility of this mechanism for the magnetic acceleration. Note that the final balance of rotation in our experiments would be made not exactly in the electron root, since the contribution from non-ambipolar ion transport is not completely ignorable. In fact, the saturation of rotation due to a 3D field can be anywhere between ion and electron root depending on the temperature of the two thermal species, especially when the initial balance of rotation without the 3D field was between the two roots.

Considering the non-ambipolar electron transport as the key mechanism, we performed two kinetic MHD simulations, using GPEC [36]and MARS-K codes [22, 37] which are both linear but uniquely self-consistent across 3D equilibrium and neoclassical transport. The codes solved the linearly perturbed radial force balance based on $\vec{\nabla}\delta p + \vec{\nabla}\cdot\delta\overleftrightarrow{\Pi} = \delta\vec{j}\times\vec{B} + \vec{j}\times\delta\vec{B}$ but by calculating the displacement $\vec{\xi}$ only ideally in GPEC and by Ohm's law in MARS-K. The non-ideal tensor pressure $\delta\overleftrightarrow{\Pi}$ must be calculated kinetically in the collisionless regime and gives the torque by non-ambipolar transport. $\delta\overleftrightarrow{\Pi}$ contributions to the force balance are generally small and

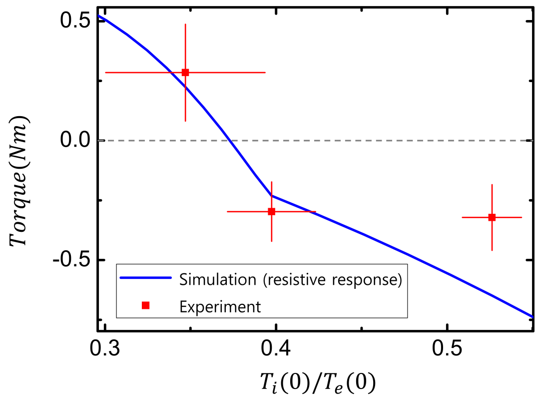

FIG. 4: (color) Comparison of measured (black, square) and calculated NTV torque with (black, solid) and without (blue, dashed) resistive response in MARS-K simulations.

ignorable in the L-mode plasmas, but becomes essential near the resonant layer to regulate $\vec{\xi}$ that otherwise becomes unrealistically large. It turns out in addition that the resistive effect is critical to amplify $\vec{\xi}$ strong enough to generate the torque measured in the experiments.

The normal displacements ξ_n calculated ideally in (a) and resistively in (b) are shown in Fig. 3, clearly illustrating the difference. Note here that the results in (a) and (c) are also based on MARS-K to be consistent but without resistivity, after the verification with GPEC calculations. The strongly amplified plasma displacements particularly around the $q = 2$ rational surface shown in (b) and (d) are due to the linear resistive field penetration but limited by non-ambipolar electron currents. Its important evidence has been obtained, by electron cyclotron emission imaging (ECEI) measurements around the $q = 2$ surface by subtracting the signal before and after $n = 1$ field application in #19118. Based on this 2D δT_e structure, ξ_n structure can be estimated by the relation $\xi_n = -\delta T_e / |\nabla T_e|$, which is applicable for $\vec{B}\cdot\nabla T_e = 0$ [35] based on the ECEI as well as separate ECE radiometers. The estimated 2D displacement structure shown in Fig. 3 (e) is indeed agreed with the simulation by resistive and kinetic 3D response (Fig. 3 (d)). Note that a magnetic surface overlap may not occur in this case, even with the peaked displacement of 20 mm, as inferred from the $|d\xi_r/dr| < 1$, thus the linear calculation could be valid.

The torque by non-ambipolar transport is then calculated by $\left\langle \hat{e}_\phi \cdot \vec{\nabla} \cdot \overleftrightarrow{\Pi} \right\rangle$ based on $\vec{\xi}$ obtained by resistive 3D response and $\delta_L \vec{B} = \vec{\nabla} \times (\vec{\xi} \times \vec{B}_0) + \vec{\xi} \cdot \vec{\nabla} \vec{B}_0$ [38]. In principle, $\overleftrightarrow{\Pi}$ should be $\overleftrightarrow{\Pi}_e + \overleftrightarrow{\Pi}_i$ including the contributions from the collisionless electrons and collisional ions, but the collisional $\overleftrightarrow{\Pi}_i$ is not included in the MARS-K model and thus done based on a simplified formula used in [14]. The calculated NTV without the resistive effect is only about $10^{-3} Nm$ for #19115, whereas the experimental torque measured from the time evolution of the angular momentum density, $\partial L/\partial t$ is in an order of $10^{-1} Nm$. This level of torque is consistent with the modified rotation against the NBI torque estimated by NUBEAM [39], which is as large as 0.55 Nm. It is the NTV simulation including the resistive field penetration that explains the empirical torque, as presented in Fig. 4. Here the simulation curve is obtained by gradually changing T_i/T_e rather than ω_ϕ. This is because theoretically T_i can better simulate the possible torque variations determined by the competition between the collisionless electrons and collisonal ions. The agreement on the leftmost experimental point demonstrates that the magnetic acceleration can be indeed explained by the self-consistent NTV with drifting electrons when the RMP is amplified by resistive field penetration. The simulation also explains the sign flip when $T_i(0)/T_e(0) \approx 0.37$, at which the two species are expected to have ambipolar transport even in the presence of non-axisymmetry. Magnetic braking in the other two experiments is also well reproduced in higher $T_i(0)/T_e(0) > 0.37$, although there is an indication of overestimated counter-I_P torques when the ion NTV becomes larger. This might be due to the collisional ion effects are calculated in a non-self-consistent fashion, and also are not including the precessional effects in the transport model.

In summary, the physics mechanism behind the magnetic acceleration and saturation observed in KSTAR RMP experiments is shown to be the non-ambipolar transport of collisionless drifting electrons towards the ambipolar level of the radial electric field, on the top of resistive field penetration and amplified 3D response. The empirically measured response by ECEI and torque during the magnetic acceleration and braking are all successfully explained by the self-consistent MARS-K simulation, indicating its predictive capability of multi-species non-ambipolar transport driven by a 3D field. The benefit of this phenomenon is also manifested during the experiments by the improved tolerance of slowly rotating plasma against LMs. An important implication is that the magnetic acceleration and its benefit on plasma stability can be predictably acquired in low torque plasmas when it becomes possible to enhance non-ambipolar electron transport, especially in high ion collisional regime as directly validated in our study or potentially in low collisionality as predicted [18].

* jpark@pppl.gov
† ysna@snu.ac.kr

[1] H Biglari, P H Diamond, and P W Terry. Influence of sheared poloidal rotation on edge turbulence. Physics of Fluids B: Plasma Physics, 2(1):1–4, 1990.
[2] T S Hahm and K H Burrell. Flow shear induced fluctu-

ation suppression in finite aspect ratio shaped tokamak plasma. Physics of Plasmas, 2(5):1648–1651, 1995.

[3] K H Burrell. Effects of EB velocity shear and magnetic shear on turbulence and transport in magnetic confinement devices. Physics of Plasmas, 4(5):1499–1518, 1997.

[4] A. M. Garofalo, E. J. Strait, L. C. Johnson, R. J. La Haye, E. A. Lazarus, G. A. Navratil, M. Okabayashi, J. T. Scoville, T. S. Taylor, and A. D. Turnbull. Sustained Stabilization of the Resistive-Wall Mode by Plasma Rotation in the DIII-D Tokamak. Physical Review Letters, 89(23):1–4, 2002.

[5] S. A. Sabbagh, R. E. Bell, J. E. Menard, D. A. Gates, A. C. Sontag, J. M. Bialek, B. P. Leblanc, F. M. Levinton, K. Tritz, and H. Yuh. Active stabilization of the resistive-wall mode in high-beta, low-rotation plasmas. Physical Review Letters, 97(4):1–4, 2006.

[6] R. J. Buttery, R. J. La Haye, P. Gohil, G. L. Jackson, H. Reimerdes, and E. J. Strait. The influence of rotation on the N threshold for the 2/1 neoclassical tearing mode in DIII-D. Physics of Plasmas, 15(5), 2008.

[7] H. R. Koslowski, Y. Liang, A. Krämer-Flecken, K. Löwenbrück, M. Von Hellermann, E. Westerhof, R. C. Wolf, and O. Zimmermann. Dependence of the threshold for perturbation field generated m/n 2/1 tearing modes on the plasma fluid rotation. Nuclear Fusion, 46(8), 2006.

[8] K. C. Shaing. Magnetohydrodynamic-activity-induced toroidal momentum dissipation in collisionless regimes in tokamaks. Physics of Plasmas, 10(5 I):1443–1448, 2003.

[9] Jong Kyu Park, Allen H. Boozer, and Jonathan E. Menard. Nonambipolar transport by trapped particles in tokamaks. Physical Review Letters, 102(6):1–4, 2009.

[10] J. D. Callen, A. J. Cole, and C. C. Hegna. Toroidal rotation in tokamak plasmas. Nuclear Fusion, 49(8), 2009.

[11] K. C. Shaing, S. A. Sabbagh, and M. S. Chu. An approximate analytic expression for neoclassical toroidal plasma viscosity in tokamaks. Nuclear Fusion, 50(2), 2010.

[12] J. D. Callen. Effects of 3D magnetic perturbations on toroidal plasmas. Nuclear Fusion, 51(9), 2011.

[13] S. Nowak, E. Lazzaro, O. Sauter, G. Canal, B. Duval, L. Federspiel, A N Karpushov, D. Kim, H. Reimerdes, J. Rossel, and D. Wagner. Evidence of Neoclassical Toroidal Viscosity on the Neoclassical Tearing Modes in {TCV} tokamak. Journal of Physics: Conference Series, 401:12017, dec 2012.

[14] W. Zhu, S. A. Sabbagh, R. E. Bell, J. M. Bialek, M. G. Bell, B. P. Leblanc, S. M. Kaye, F. M. Levinton, J. E. Menard, K. C. Shaing, A. C. Sontag, and H. Yuh. Observation of plasma toroidal-momentum dissipation by neoclassical toroidal viscosity. Physical Review Letters, 96(22):1–4, 2006.

[15] A. J. Cole, J. D. Callen, W. M. Solomon, A. M. Garofalo, C. C. Hegna, M. J. Lanctot, and H. Reimerdes. Observation of peak neoclassical toroidal viscous force in the DIII-D tokamak. Physical Review Letters, 106(22):1–4, 2011.

[16] J. K. Park, Y. M. Jeon, J. E. Menard, W. H. Ko, S. G. Lee, Y. S. Bae, M. Joung, K. I. You, K. D. Lee, N. Logan, K. Kim, J. S. Ko, S. W. Yoon, S. H. Hahn, J. H. Kim, W. C. Kim, Y. K. Oh, and J. G. Kwak. Rotational resonance of nonaxisymmetric magnetic braking in the KSTAR tokamak. Physical Review Letters, 111(9):1–4, 2013.

[17] R. V. Budny. Comparisons of predicted plasma performance in ITER H-mode plasmas with various mixes of external heating. Nuclear Fusion, 49(8), 2009.

[18] Y Sun, Y Liang, K C Shaing, H R Koslowski, C Wiegmann, and T Zhang. Modelling of the neoclassical toroidal plasma viscosity torque in tokamaks. Nuclear Fusion, 51(5), 2011.

[19] S. A. Sabbagh, Y. S. Park, J Kim, W. H. Ko, S. H. Hahn, Y In, Y. K. Oh, K. C. Shaing, and Y Sun. Observation of the Generalized Neoclassical Toroidal Viscosity Offset Rotation Profile in KSTAR. In APS Meeting Abstracts, page NO4.007, 2017.

[20] S A Sabbagh, Y S Park, J Kim, J Ko, W H Ko, Ker-Chung Shaing, Y Sun, S H Hahn, Y In, Y M Jeon, H H Lee, J H Lee, S G Lee, Y K Oh, J Seol, and J W Yoo. Observation of the generalized neoclassical toroidal viscosity offset rotation profile and implications for ITER. In A Bret, M Fajardo, E Westerhof, A Melzer, B Dromey, and C Riconda, editors, 44th EPS Conference on Plasma Physics, EPS 2017, 44th EPS Conference on Plasma Physics, EPS 2017. European Physical Society (EPS), jan 2017.

[21] F. Imbeaux, J. Citrin, J. Hobirk, G. M.D. Hogeweij, F. Köchl, V. M. Leonov, S. Miyamoto, Y. Nakamura, V. Parail, G. Pereverzev, A. Polevoi, I. Voitsekhovitch, V. Basiuk, R. Budny, T. Casper, J. Fereira, A. Fukuyama, J. Garcia, Y. V. Gribov, N. Hayashi, M. Honda, I. H. Hutchinson, G. Jackson, A. A. Kavin, C. E. Kessel, R. R. Khayrutdinov, C. Labate, X. Litaudon, P. J. Lomas, J. Lönnroth, T. Luce, V. E. Lukash, M. Mattei, D. Mikkelsen, I. Nunes, Y. Peysson, P. Politzer, M. Schneider, G. Sips, G. Tardini, S. M. Wolfe, and V. E. Zhogolev. Current ramps in tokamaks: From present experiments to ITER scenarios. Nuclear Fusion, 51(8), 2011.

[22] Yueqiang Liu, M S Chu, I T Chapman, and T C Hender. Toroidal self-consistent modeling of drift kinetic effects on the resistive wall mode. Physics of Plasmas, 15(11), 2008.

[23] Y. M. Jeon, J. K. Park, S. W. Yoon, W. H. Ko, S. G. Lee, K. D. Lee, G. S. Yun, Y. U. Nam, W. C. Kim, Jong Gu Kwak, K. S. Lee, H. K. Kim, and H. L. Yang. Suppression of edge localized modes in high-confinement KSTAR plasmas by nonaxisymmetric magnetic perturbations. Physical Review Letters, 109(3):1–5, 2012.

[24] J.-K. Park, Y. M. Jeon, Y. In, J. W. Ahn, R. Nazikian, G. Y. Park, J. H. Kim, H. H. Lee, W. H. Ko, H.-S. Kim, N. C. Logan, Z. Wang, E. A. Feibush, J. E. Menard, and M. C. Zarnstorff. 3D field phase-space control in tokamak plasmas. Nature Physics, 14:1223–1228, 2018.

[25] T. C. Hender, R. Fitzpatrick, A. W. Morris, P. G. Carolan, R. D. Durst, T. Edlington, J. Ferreira, S. J. Fielding, P. S. Haynes, J. Hugill, I. J. Jenkins, R. J. La Haye, B. J. Parham, D. C. Robinson, T. N. Todd, M. Valovic, and G. Vayakis. Effect of resonant magnetic perturbations on COMPASS-C tokamak discharges. Nuclear Fusion, 32(12):2091–2117, 1992.

[26] Won Ha Ko, Hyungho Lee, Dongcheol Seo, and Myeun Kwon. Charge exchange spectroscopy system calibration for ion temperature measurement in KSTAR. Review of Scientific Instruments, 81(10):1–4, 2010.

[27] R. Fitzpatrick. Nonlinear error-field penetration in low density ohmically heated tokamak plasmas. Plasma Physics and Controlled Fusion, 54(9), 2012.

[28] R. J. La Haye, A. W. Hyatt, and J. T. Scoville. Nonlinear instability to low m,n=1 error fields in DIII-D as a func-

tion of plasma fluid rotation and beta. Nuclear Fusion, 32(12):2119–2126, 1992.

[29] E Lazzaro, R J Buttery, T C Hender, P Zanca, R Fitzpatrick, M Bigi, T Bolzonella, R Coelho, M DeBenedetti, S Nowak, O Sauter, and M Stamp. Error field locked modes thresholds in rotating plasmas, anomalous braking and spin-up. Physics of Plasmas, 9(9):3906, 2002.

[30] Jong Kyu Park, Jonathan E. Menard, Stefan P. Gerhardt, Richard J. Buttery, Steve A. Sabbagh, Ronald E. Bell, and Benoit P. Leblanc. Sensitivity to error fields in NSTX high β plasmas. Nuclear Fusion, 52(2), 2012.

[31] M. J. Lanctot, J.-K. Park, P. Piovesan, Y. Sun, R. J. Buttery, L. Frassinetti, B. A. Grierson, J. M. Hanson, S. R. Haskey, Y. In, Y. M. Jeon, R. J. La Haye, N. C. Logan, L. Marrelli, D. M. Orlov, C. Paz-Soldan, H. H. Wang, and E. J. Strait. Impact of toroidal and poloidal mode spectra on the control of non-axisymmetric fields in tokamaks. Physics of Plasmas, 24(5):056117, 2017.

[32] S. M. Yang, J.-K. Park, Y In, J Lee, W.H. Ko, J. Yoo, S. Hong, K. Lee, Y. Shi, S. Lee, J.W. Juhn, S.-W. Yoon, and Y.-S. Na. Effects of momentum transport on error field threshold observed in KSTAR. In APS Meeting Abstracts, page NO5.011, 2018.

[33] R. Fitzpatrick. Interaction of tearing modes with external structures in cylindrical geometry (plasma). Nuclear Fusion, 33(7):1049–1084, 1993.

[34] Y. Sun, Y. Liang, K. C. Shaing, H. R. Koslowski, C. Wiegmann, and T. Zhang. Neoclassical toroidal plasma viscosity torque in collisionless regimes in tokamaks. Physical Review Letters, 105(14):1–4, 2010.

[35] N. M. Ferraro, T. E. Evans, L. L. Lao, R. A. Moyer, R. Nazikian, D. M. Orlov, M. W. Shafer, E. A. Unterberg, M. R. Wade, and A. Wingen. Role of plasma response in displacements of the tokamak edge due to applied non-axisymmetric fields. Nuclear Fusion, 53(7), 2013.

[36] Jong Kyu Park and Nikolas C. Logan. Self-consistent perturbed equilibrium with neoclassical toroidal torque in tokamaks. Physics of Plasmas, 24(3), 2017.

[37] Z. R. Wang, M. J. Lanctot, Y. Q. Liu, J. K. Park, and J. E. Menard. Three-dimensional drift kinetic response of high-β plasmas in the DIII-D tokamak. Physical Review Letters, 114(14):1–5, 2015.

[38] Allen H. Boozer. Perturbation to the magnetic field strength. Physics of Plasmas, 13(4):1–4, 2006.

[39] Alexei Pankin, Douglas McCune, Robert Andre, Glenn Bateman, and Arnold Kritz. The tokamak Monte Carlo fast ion module NUBEAM in the national transport code collaboration library. Computer Physics Communications, 159(3):157–184, 2004.